

# Multifaceted Study of CuTCNQ Thin-Film Materials. Fabrication, Morphology, and Spectral and Electrical Switching Properties

Sheng-Gao Liu, Yun-Qi Liu, Pei-Ji Wu, and Dao-Ben Zhu\*

*Institute of Chemistry, Chinese Academy of Sciences, Beijing 100080, China*

Received May 7, 1996. Revised Manuscript Received August 16, 1996<sup>8</sup>

A series of CuTCNQ (TCNQ = 7,7,8,8-tetracyano-*p*-quinodimethane) thin-film materials were prepared by different methods or under different conditions and characterized by scanning electron microscopic analyses, infrared, Raman, and UV-vis spectral analyses, and current–voltage characteristic measurements. All of the spectral analyses were compared with those of chemically synthesized pure CuTCNQ powder produced by the metathetical reaction of CuI and TCNQ. The effects of the preparation methods or growth parameters upon the morphology of the film materials and their physical properties were discussed.

## 1. Introduction

Since Potember et al.<sup>1</sup> reported bistable, reproducible, and nanosecond electrical switching in an organometallic charge-transfer (CT) complex CuTCNQ (TCNQ = 7,7,8,8-tetracyano-*p*-quinodimethane), electrical, optical, and optoelectronic switches have been demonstrated by many different authors,<sup>2–8</sup> and furthermore the switching effect in CuTCNQ films has been frequently referred to as a prototype of a molecular electronic device. These materials undergo electrical switching as well as phototransformation phenomena under the influence of an electric field<sup>2</sup> or a laser beam.<sup>6,9</sup> Such kinds of properties make these materials promising candidates for useful technological applications, of which erasable photochromatic laser disk and a series memories (RAM or ROM) have been shown the most interest.<sup>2</sup> However, there are still many fundamental problems to be solved. These involve (1) the switching effect is dependent on or independent of the polarity of the applied potentials; (2) the threshold voltage ( $V_{th}$ ) is dependent on or independent of the film thickness; and so on. For example, Potember et al.<sup>1</sup> did not observe the polarization dependence of the switching phenomena. But Sato et al.<sup>10</sup> observed the polarized memory effects. The differences between Sato's fabrication process and Potember's are (1) Sato et al. used the mixed solvent for the preparation of CuTCNQ films, (2) the TCNQ solution was not saturated with TCNQ but rather diluted with

a concentration of about 1 mM, (3) Sato et al. prepared the copper electrode by evaporation under vacuum and treated its surface with hydrofluoric acid in advance of the reaction with TCNQ.

To better understand the properties of this interesting material and to resolve some of the questions surrounding the behavior of Al–CuTCNQ–Cu devices, a multifaceted study on the fabrication, morphology, spectral, and electrical properties of the thin-film materials is required. In this contribution, we focus our attention on some experimental aspects of these materials and pay our attention to the role played by the fabrication process of the CuTCNQ films in determining their morphologies and further to the role played by the morphology in determining the spectral characteristics of the film materials and the electronic properties of the complete devices. We demonstrate here that changing the preparation methods or growth parameters can significantly change the morphology of the resulting CuTCNQ films; however, these morphological changes do not lead to significant changes in the spectral characteristics of the films and the electronic properties of the complete Al–CuTCNQ–Cu devices.

## 2. Experimental Section

TCNQ, purchased from Aldrich, was recrystallized twice from purified and degassed acetonitrile and then sublimed onto Teflon under vacuum before use. CuTCNQ polycrystalline powder was synthesized as described by Melby et al.<sup>11</sup> All CuTCNQ films studied here were grown on pure copper substrates, which were made from high-purity copper strip (2 × 1 cm<sup>2</sup>). The strip was first polished by using metallographic polishing paper from 0 down to 4/0, followed by cleaning with solvents to remove sanding particles and organics from the surface and then cleaned by dipping in 1:1 HNO<sub>3</sub> aqueous solution, finally washed, dried, and used immediately to grow CuTCNQ films.

Film produced by the solid-state spontaneous redox reaction of copper and molten TCNQ and by the vapor deposition of TCNQ on a copper surface under vacuum were prepared as described in the literatures.<sup>12–14</sup>

<sup>8</sup> Abstract published in *Advance ACS Abstracts*, October 1, 1996.  
 (1) Potember, R. S.; Pochler, T. O.; Cowan, D. O. *Appl. Phys. Lett.* **1979**, *34*, 405.  
 (2) Hua, Z. Y.; Chen, G. R. *Vacuum* **1992**, *43*, 1019.  
 (3) Potember, R. S.; Pochler, T. O.; Rappa, A.; Cowan, D. O.; Bloch, A. N. *J. Am. Chem. Soc.* **1980**, *102*, 3659.  
 (4) Potember, R. S.; Pochler, T. O.; Benson, R. C. *Appl. Phys. Lett.* **1982**, *41*, 548.  
 (5) Benson, R. C.; Hoffman, R. C.; Potember, R. S.; Bourkoff, E.; Pochler, T. O. *Appl. Phys. Lett.* **1983**, *42*, 855.  
 (6) Kamitsos, E. I.; Risen, W. M. *Solid State Commun.* **1983**, *45*, 165.  
 (7) Hoshino, H.; Matsushita, S.; Samura, H. *Jpn. J. Appl. Phys.* **1986**, *25*, L341.  
 (8) Hoffman, R. C.; Potember, R. S. *Appl. Opt.* **1989**, *28*, 1417.  
 (9) Potember, R. S.; Pochler, T. O.; Benson, R. C. U.S. Patent **1986**, 4,574,366.  
 (10) Sato, C.; Wakamatsu, S.; Tadokoro, K. *J. Appl. Phys.* **1990**, *68*, 6535.

(11) Melby, L. R.; Harder, R. J.; Hertler, W. R.; Mahler, W.; Benson, R. E.; Mochel, W. E. *J. Am. Chem. Soc.* **1962**, *84*, 3374.

**Table 1. Preparation Conditions of CuTCNQ Film Materials with the Dimensions of the Rods in Polycrystalline Samples**

film or sample	length (μm)	width (μm)	solvent	concn (mM)	time (min)	temp (°C)
1 <sup>a</sup>	3.5–5.5	0.5–1.7	acetonitrile	50	1	80
2 <sup>a</sup>	4	1.4	acetonitrile	50	2	80
3 <sup>a</sup>	6	2.0	acetonitrile	50	4	80
4 <sup>a</sup>	6–7	2.0–2.5	acetonitrile	50	6	80
5 <sup>a</sup>	8	1.7	acetonitrile	50	8	80
6 <sup>a</sup>	10	3	acetonitrile	50	10	80
7 <sup>a</sup>	6	2–4	acetonitrile	10	6	80
8 <sup>a</sup>	6	3.5	acetonitrile	5	6	80
9 <sup>a</sup>	7	6–7	acetonitrile	5	7	80
10 <sup>a</sup>	5	0.5	acetonitrile	saturated <sup>b</sup>	14	room temp (11)
11 <sup>c</sup>			chlorobenzene	50	1	120
12	7	0.3	1-bromohexadecane	50	1	180
13	3.5	0.2			0.3	240
14 <sup>d</sup>					0.3	296

<sup>a</sup> Polycrystalline. <sup>b</sup> The concentration of the saturated solution is about 2 mM. <sup>c</sup> Amorphous containing nanometer-sized (50–200 nm) CuTCNQ particles.<sup>15</sup> <sup>d</sup> Amorphous.<sup>14</sup>

General descriptions for the preparation of solution-grown CuTCNQ films were as follows. A copper metal surface, as treated above, was combined with a 20–50 mL solution of a definite concentration of TCNQ in an appropriate solvent (acetonitrile, chlorobenzene, or 1-bromohexadecane) for a desired amount of time at a definite temperature. The preparation conditions for each sample are given in Table 1. After the desired amount of time, the Cu–CuTCNQ bilayer was removed and gently rinsed with the solvent and then allowed to dry under vacuum. The solution was not stirred during the film growth. All of the solvents used were purified and degassed prior to their use according to standard methods.

Scanning electron microscopy (SEM) was done using a Hitachi S530 microscopy. The accelerator voltage was 25 keV with a working distance of about 10 mm.

Small-angle X-ray diffraction (SAXRD) measurements were carried out at room temperature on a Dmax-3B diffractometer using a Cu K $\alpha$  radiation. The X-ray source was operated at 40 kV and 30 mA. Scan speed was 2°/min.

UV-vis spectra were recorded on a Hitachi 340 spectrophotometer in acetonitrile solution.

FT-IR spectra were recorded on a Bruker IFS-113V fourier transform infrared spectrophotometer in the region 4000–500  $\text{cm}^{-1}$  as KBr pellets. The spectral accuracy and resolution was 2  $\text{cm}^{-1}$  or better.

Microreflectance FT-IR spectra were recorded on a Nicolet Magna IR 750 Fourier transform infrared spectrophotometer equipped with a Nic-Plan IR microscope in the region 4000–650  $\text{cm}^{-1}$  with 500 scans. The spectral accuracy and resolution was better than 1.0  $\text{cm}^{-1}$ .

Raman spectra were recorded on a Nicolet Raman 910 spectrophotometer equipped with a Nd:YVO<sub>4</sub> laser (1064 nm) in the region 4000–100  $\text{cm}^{-1}$  with 1000 scans and power less than 160 mW (<5000 mW  $\text{cm}^{-2}$ ). Since the light-induced transformations of stationary CuTCNQ samples were reported in the initial state of the film when the Raman source power exceeded certain threshold values, careful control of source power was employed to measure the spectra of the untransformed CuTCNQ samples. The spectral accuracy and resolution were better than 1.0  $\text{cm}^{-1}$ .

For electrical measurements, top metal electrode of aluminum was evaporated onto the surface of the film under vacuum forming 1 mm × 1 mm contacts. The electrical measurements were performed in air at room temperature.

### 3. Results and Discussion

#### 3.1. Materials and Morphology.

CuTCNQ films used in this study were prepared by three different

methods. The first method is the solution one employed by Potember et al.,<sup>1</sup> which is based on the fact that solutions of TCNQ react with metallic copper by a spontaneous redox reaction that forms dark blue microcrystals of CuTCNQ on the surface of the copper substrate.<sup>1</sup> This “wet” method is the most often used, although different authors sometimes chose different concentrations of TCNQ, different solvents, various copper substrate cleaning methods, or different reaction times and temperatures. We did not attempt, therefore, to make morphological, spectral, and electrical measurements on films prepared at every possible point on the times, concentrations, solvents, temperatures, and copper substrate cleaning methods. Rather we chose a fixed copper substrate cleaning method and observed the effects of solvents, concentrations, reaction times, and temperatures. The second method, newly developed by us, is a “dry” method based on that molten TCNQ react with copper by a solid-state redox reaction under highly pure nitrogen atmosphere that forms large blocks of CuTCNQ on the surface of the copper substrate.<sup>14</sup> The remainder of our CuTCNQ film was prepared by vapor deposition of TCNQ on copper substrate under vacuum at a high temperature. Table 1 tabulates the CuTCNQ film materials studied with the preparation conditions for each sample and the dimensions of the rods in polycrystalline samples. Films **1–12** were grown in solutions using acetonitrile or chlorobenzene or 1-bromohexadecane as the solvent. Film **13** was prepared by vapor deposition of TCNQ upon the surface of the copper substrate under vacuum at around 240 °C. Film **14** was produced by dipping a copper substrate into molten TCNQ forming tightly packed large blocks of CuTCNQ.<sup>14</sup> Films **11** and **14** are amorphous; the others are polycrystalline.

**3.2. Effects of the Growth Parameters on the Morphology of the Solution-Grown CuTCNQ Films.** First, we investigate the effects of different solvents on the morphology of the solution-grown films. As shown in Table 1, we can notice that all the films (**1–10, 12**) grown in both acetonitrile and 1-bromohexadecane were polycrystalline; however, the film (**11**) grown in chlorobenzene is amorphous.<sup>15</sup> Furthermore, the diameter of the particles lies in 50–200 nm. This nanometer feature makes the film very interesting to be investigated the physical properties.<sup>15</sup> Figure 1 shows SEM

(12) Liu, S. G.; Liu, Y. Q.; Wu, P. J.; Zhu, D. B. *Chem. J. Chin. Univ.* **1995**, *16* (suppl. 11), 159.

(13) Li, X. L.; Wu, P. J.; Zhu, D. B., unpublished work.

(14) Liu, S. G.; Liu, Y. Q.; Wu, P. J.; Zhu, D. B. *Thin Solid Films*, in press.

(15) Liu, S. G.; Liu, Y. Q.; Zhu, D. B. *Thin Solid Films*, in press.

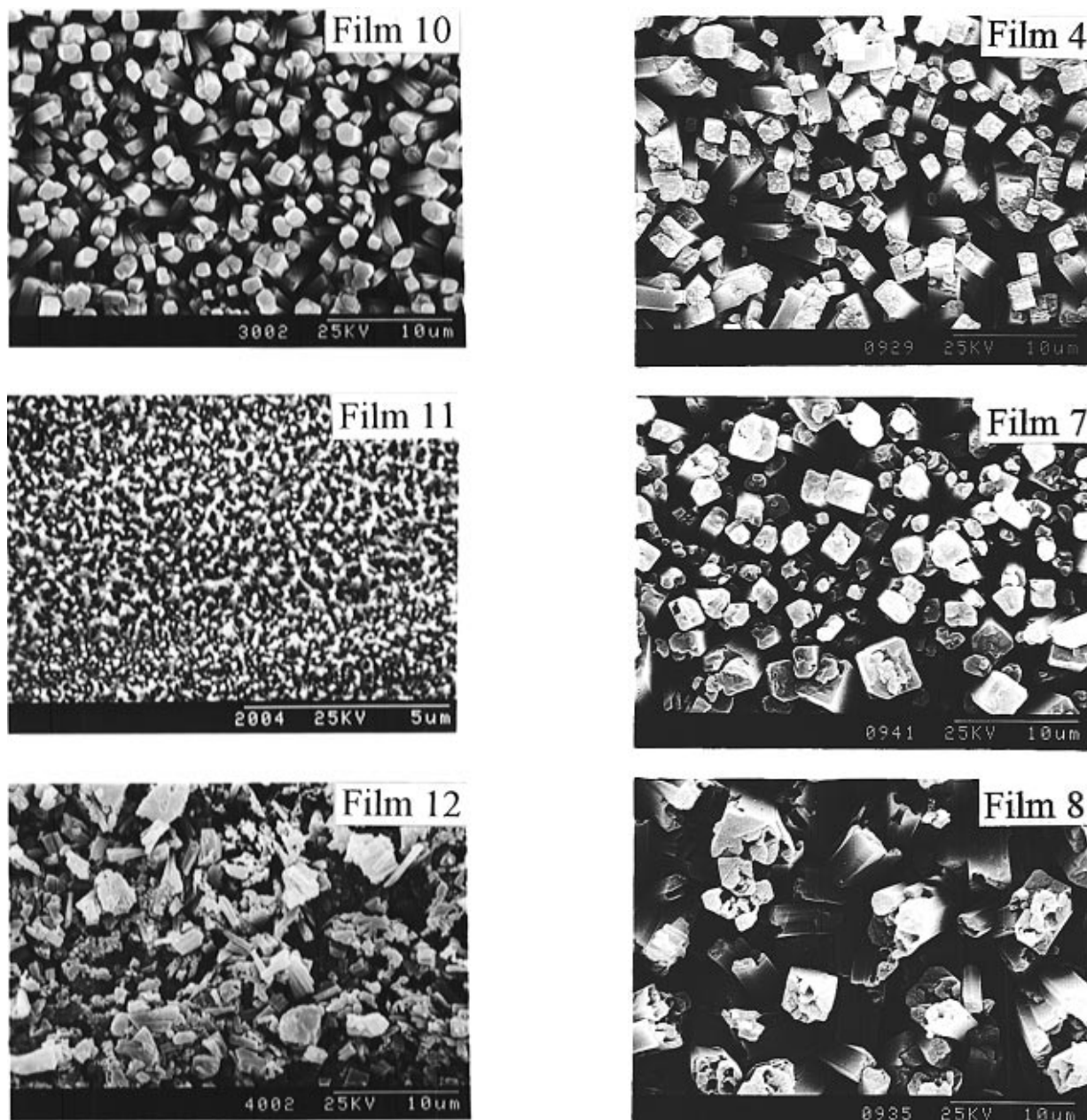


**Figure 1.** SEM graphs of the solution-grown films **10**, **11**, and **12** in different solvents.

micrographs of three typical films grown in acetonitrile at room temperature, chlorobenzene at 120 °C, and 1-bromohexadecane at 180 °C, respectively, at fixed concentrations of TCNQ (50 mM) except for that grown at room temperature.

Second, we investigate the effect of the concentrations of TCNQ on the morphology of the solution-grown CuTCNQ films. Figure 2 shows SEM micrographs of three typical films, **4**, **7**, and **8**, grown in 50, 10, and 5 mM acetonitrile solution for 6 min at 80 °C. The structure of the films consists of long rods, ranging from 6 to 7  $\mu$ m in length and 2 to 4  $\mu$ m in width, oriented roughly normal to the surface and loosely packed. Furthermore, as the concentration decreased from 50, 10 to 5 mM, the structure of the film becomes looser. In addition, all the films (**4**, **7**, and **8**) appear to be roughly mosaic structures, and with the decrease of the concentration, the mosaic nature is reduced. Thus, this structure can be hardly observed in the case of the film **8**, which was grown in 5 mM acetonitrile solution (see

**Figure 2.** SEM graphs of the solution-grown films **4**, **7**, and **8** by varying the concentrations from 50, 10, to 5 mM in acetonitrile.

Figure 2). Another evident trend was observed, that is, with decreasing concentrations of TCNQ in acetonitrile solution, the long rods became hollow. This trend can be enhanced by increasing the exposure time at fixed temperatures and concentrations.

Time effects can be reflected by Figure 3, which is composed of SEM micrographs taken of the films **1–3**, **5**, and **6** produced by reaction at the same temperatures and concentrations for 1–10 min in acetonitrile. We can notice that film **1**, which was produced at the temperature and concentration for 1 min, appears to be more loosely packed than those exposed for a longer time. However, the films exposed for more than 2 min again become more loosely packed than the film **2**, which is produced at the temperature and concentration for 2 min.

Comparing Figures 2 and 3, one can notice that there are two typical different structures in the polycrystalline

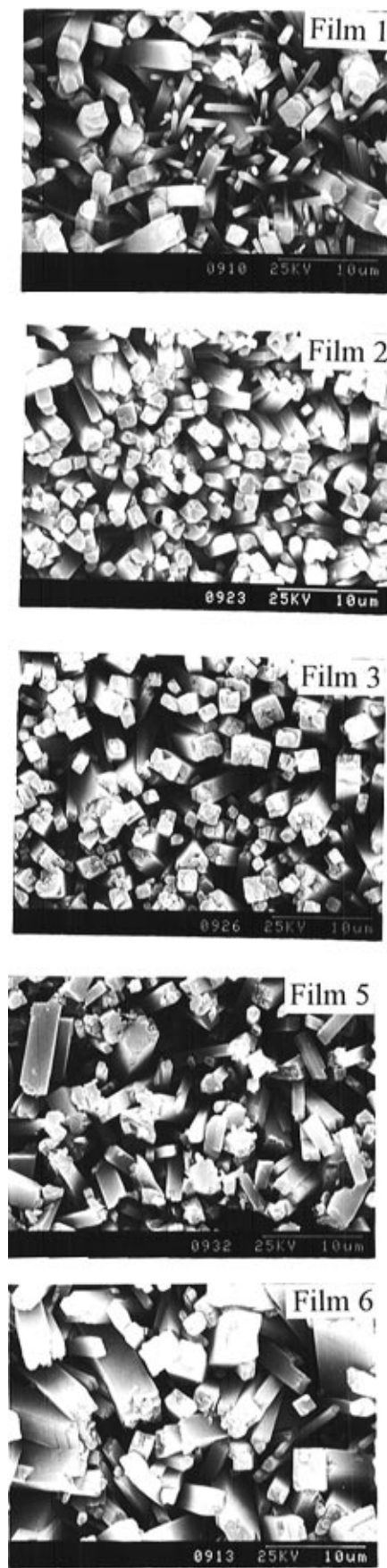


**Figure 3.** SEM graphs of the films **1**, **2**, **3**, **5**, and **6** with the increase of exposure time from 1 to 10 min.

film materials. One is a mosaic structure, and the other is not a mosaic structure. The difference in the two kinds of morphologies probably arises from the partial

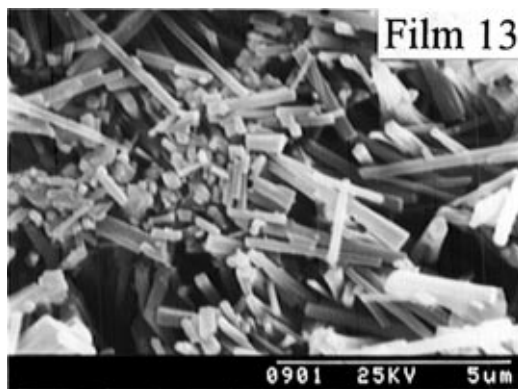


**Figure 4.** SEM graph of the film **13** produced by vapor deposition of TCNQ on copper surface under vacuum at around 240 °C.

solubility of CuTCNQ in the acetonitrile solvent.<sup>16</sup> As the CuTCNQ grows, part of it redissolves into the solvent. After a definite period of time, the saturation point of CuTCNQ in solution is reached, forcing CuTCNQ in solution to deposit onto the growing layer of CuTCNQ. The net effect is to cause the rods to coalesce into the mosaic structure.<sup>17</sup> This process can be followed by looking at a series of different time exposures; see Figure 3. At short times (1–2 min) there are almost only rods present, but, as the time of exposure is increased from 4 to 10 min, it is apparent that the rods are slowly coalescing into the mosaic structure. While the pictures show the results of varying time at fixed temperatures and concentrations, similar results were obtained by holding the exposure time constant and varying the temperature. Thus, it is better for us to control the time of exposure to about 2 min at 80 °C or to about 10 min at room temperature to avoid forming the mosaic structure.

All of the films mentioned above were produced by the "wet" method, i.e., the films were grown in solutions. On the other hand, "dry" methods such as physical vapor deposition and molecular beam epitaxy are preferable because these methods are capable of avoiding the contamination from the preparation solution. As a result, films formed by vapor deposition of TCNQ on copper under vacuum and by contacting copper with molten TCNQ were investigated and compared to the solution-grown ones.<sup>14</sup> Figure 4 shows the SEM graph of sample **13** formed by vapor deposition. The crystal size was smaller and relatively uniform as compared with earlier reported results,<sup>18</sup> and they were in the range of crystal size of about 3.5 μm in length and 0.2 μm in width. Furthermore, the crystallinity of the film is much worse than that of the solution-grown film; see Figure 5. This is very important for some practical purposes since small crystallites are necessary for the film, especially for a high density of recording system.

**3.3. Spectral Characterization.** *3.3.1. Infrared Spectral Characteristics.* Table 2 presents the characteristic infrared absorptions of films **1**–**13** as well as the synthesized pure CuTCNQ powder and pure TCNQ. Table 2 shows that for the CuTCNQ films, spectra

(16) Duan, H.; Cowan, D. O.; Kruger, J. *Mater. Res. Symp. Proc.* **1990**, *173*, 165.

(17) Hoagland, J. J.; Wang, X. D.; Hipps, K. W. *Chem. Mater.* **1993**, *5*, 54.

(18) Hoffman, R. C.; Potember, R. S. *Appl. Opt.* **1989**, *28*, 1417.

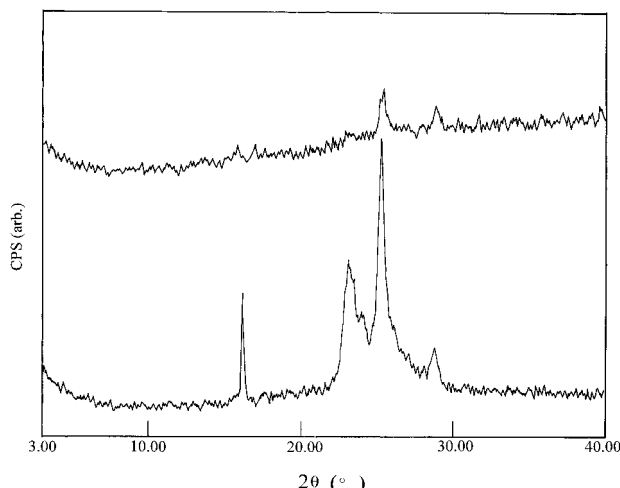


**Figure 5.** SAXRD patterns of the films **12** (bottom) and **13** (upper) with the peaks tabulated as follows:

material	2θ (deg)	d	intensity
film <b>12</b> <sup>a</sup>	16.18	5.473	203
	23.14	3.84	250
	24.12	3.686	172
	25.26	3.522	417
	28.80	3.097	126
	16.98	5.217	87
film <b>13</b>	25.18	3.533	150
	25.42	3.501	165
	28.94	3.082	138

<sup>a</sup> SAXRD pattern of the film **12** showed sharp diffraction peaks, indicating good crystallinity of the microcrystals.

different from that of TCNQ were obtained. However, the differences among the films **1–13** and the synthesized CuTCNQ powder are rather small. This means that changing the preparation methods or growth parameters does not change the IR spectral characteristics of the resulting CuTCNQ films. For the CuTCNQ films, the C≡N stretching region was characterized by three bands, maxima at about  $2198 \pm 1$  and two shoulders at around  $2171 \pm 2$  and  $2164 \pm 2 \text{ cm}^{-1}$  and the C=C ring stretching region was characterized by two bands, a weak absorption at  $1576\text{--}1577 \text{ cm}^{-1}$  and a middle one at  $1506\text{--}1507 \text{ cm}^{-1}$ . The appearance of the middle absorption peak at  $1506\text{--}1507$  indicates that TCNQ was changed to TCNQ anion radicals. The C=C wing stretching region was also characterized by two bands at around  $1352 \pm 1$  and  $1330\text{--}1331 \text{ cm}^{-1}$ , respectively, for all of the CuTCNQ films **1–13**. In conclusion, comparing the spectra of pure TCNQ, the C=C ring stretching mode in the pure TCNQ at  $1544 \text{ cm}^{-1}$  was split into about  $1576$  and  $1507 \text{ cm}^{-1}$  in both the synthesized pure CuTCNQ powder and the CuTCNQ films and the C=C wing stretching mode in the pure TCNQ at  $1353 \text{ cm}^{-1}$  was shifted to  $1359 \text{ cm}^{-1}$  in the synthesized pure CuTCNQ powder and split into two bands at about  $1352$  and  $1330 \text{ cm}^{-1}$  in the CuTCNQ films respectively. The peak of C=C–H bending at  $862 \text{ cm}^{-1}$  in the pure TCNQ was shifted to about  $826 \text{ cm}^{-1}$  in both the synthesized pure CuTCNQ powder and the CuTCNQ films. Other weak peaks at around  $1220$ ,  $1180$ ,  $1015$ , and  $990 \text{ cm}^{-1}$  in the spectra of the film materials and the CuTCNQ powder may be synergistic absorptions of both C=C stretching and C=C–H bending.

**3.3.2. UV–Vis Spectral Characteristics.** It is known that the electronic transitions in TCNQ-based CT

**Table 2. Some Selected IR Absorptions<sup>a</sup> of the CuTCNQ Film Materials, Pure TCNQ, and the Synthesized CuTCNQ Powder**

film or sample	C≡N stretching	C=C ring stretching	C=C wing stretching	C–H bending out-of-plane
1	2198 (s)	1576 (w)	1352 (m)	826 (w)
	2171 (sh, m)	1507 (m)	1330 (m)	
	2165 (sh, m)			
2	2199 (s)	1576 (w)	1352 (m)	826 (w)
	2170 (sh, w)	1507 (m)	1330 (m)	
	2164 (sh, w)			
3	2198 (s)	1576 (w)	1352 (m)	826 (w)
	2173 (sh, m)	1507 (m)	1330 (m)	
	2165 (sh, m)			
4	2198 (s)	1576 (w)	1352 (m)	826 (w)
	2173 (sh, w)	1507 (m)	1330 (m)	
	2164 (sh, w)			
5	2198 (s)	1576 (w)	1352 (m)	826 (w)
	2172 (sh, w)	1507 (m)	1331 (m)	
	2163 (sh, w)			
6	2199 (s)	1576 (w)	1352 (m)	826 (w)
	2172 (sh, w)	1507 (m)	1330 (m)	
	2165 (sh, w)			
7	2198 (s)	1576 (w)	1352 (m)	826 (w)
	2171 (sh, w)	1507 (m)	1331 (m)	
	2164 (sh, w)			
8	2199 (s)	1576 (w)	1352 (m)	826 (w)
	2172 (sh, w)	1507 (m)	1330 (m)	
	2165 (sh, w)			
9	2199 (s)	1576 (w)	1352 (m)	826 (w)
	2172 (sh, w)	1507 (m)	1330 (m)	
	2165 (sh, w)			
10	2199 (s)	1576 (w)	1353 (m)	826 (w)
	2172 (sh, w)	1507 (m)	1330 (m)	
	2166 (sh, w)			
11 <sup>b</sup>	2199 (vs)	1577 (w)	1353 (w)	826 (w)
	2174 (w)	1506 (m)	1331 (w)	
12	2197 (s)	1576 (w-m)	1351 (m)	826 (w)
	2167 (w)	1506 (m)	1330 (m)	
13	2199 (vs)	1577 (w)	1352 (m)	825 (w)
	2174 (sh, m)	1506 (m)	1339 (m)	
CuTCNQ	2208 (vs)	1576 (vw)	1359 (m)	825 (s)
	2172 (m)	1506 (m)		
TCNQ	2227 (s)	1544 (s)	1353 (m)	862 (vs)

<sup>a</sup> vs: very strong, s: strong, m: middle, w: weak, vw: very weak. <sup>b</sup> Microreflectance IR absorption spectra.

compounds can be divided into two types. First, the intramolecular or localized LE<sub>1</sub> and LE<sub>2</sub> transitions correspond to the red (550–900 nm) and blue (350–550 nm) band systems respectively of isolated TCNQ anion radical. They are both polarized in the molecular plane. Second, the intermolecular or CT transitions (CT<sub>1</sub> and CT<sub>2</sub>) lie in the red-band region. CT<sub>1</sub> is the CT transition between two TCNQ anion radicals and CT<sub>2</sub> is the CT transition from TCNQ anion radical to TCNQ<sup>0</sup>. Both CT<sub>1</sub> and CT<sub>2</sub> are polarized in the direction perpendicular to the molecular plane.<sup>19</sup> Therefore, for a simple 1:1 salt of TCNQ with complete CT from donor to TCNQ, such as LiTCNQ, the spectra show the LE<sub>1</sub>, LE<sub>2</sub>, and CT<sub>1</sub> transitions,<sup>19</sup> and their electronic structure is dominated by the properties of the dimer type of (TCNQ)<sub>2</sub><sup>2-</sup> species.<sup>20</sup> On the contrary, simple 1:1 compounds with incomplete CT, both CT<sub>1</sub> and CT<sub>2</sub> transitions together with the corresponding LE<sub>1</sub> and LE<sub>2</sub> localized transitions can be observed.<sup>20</sup>

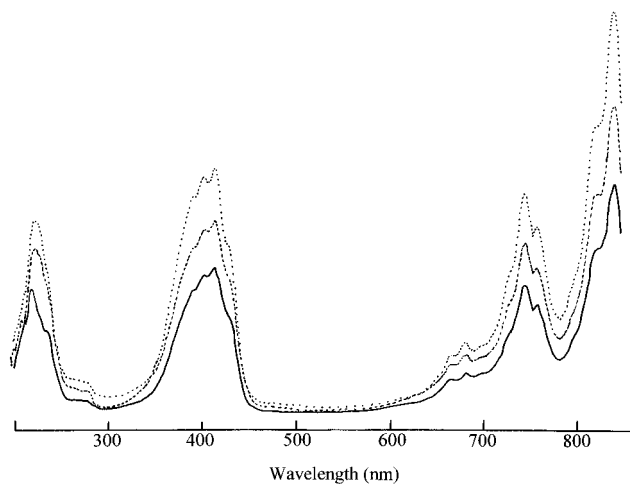
Table 3 tabulates the electronic absorptions of some selected CuTCNQ film materials and the synthesized pure CuTCNQ powder as well as pure TCNQ in acetone-

(19) Iida, Y. *Bull. Chem. Soc. Jpn.* **1969**, 42, 71.

(20) Kamitsos, E. I.; Papavassiliou, G. C.; Karakassides, M. A. *Mol. Cryst. Liq. Cryst.* **1986**, 134, 43.

**Table 3. UV–Vis Absorptions of Some Selected CuTCNQ Film Materials and Some Related Compounds in Acetonitrile Solution with Relative Absorbance to the Band at about 840 nm in Parentheses**

film	blue band ( $\lambda_{\text{max}}$ , nm)				red band ( $\lambda_{\text{max}}$ , nm)			
1	217(0.52)	235(0.34)	264(0.05)	278(0.05)	664(0.13)	680(0.17)	700(0.16)	728(0.34)
	390(0.52)	402(0.59)	414(0.62)	429(0.43)	744(0.54)	758(0.46)	820(0.70)	840(1.0)
2	228(0.41)		266(0.04)	278(0.05)	664(0.15)	680(0.19)	698(0.18)	726(0.35)
	390(0.54)	402(0.60)	414(0.63)		744(0.57)	757(0.48)	820(0.75)	840(1.0)
3	222(0.47)	236(0.33)	264(0.08)	278(0.07)	664(0.14)	680(0.17)	700(0.17)	728(0.35)
	390(0.54)	402(0.59)	414(0.61)	429(0.42)	744(0.55)	758(0.46)	820(0.71)	839(1.0)
4	219(0.52)	236(0.36)	264(0.06)	280(0.05)	664(0.14)	680(0.17)	700(0.17)	728(0.34)
	390(0.57)	402(0.61)	415(0.61)	430(0.41)	744(0.54)	758(0.46)	820(0.70)	840(1.0)
5	228(0.48)		266(0.04)	278(0.06)	664(0.16)	680(0.20)	698(0.19)	726(0.36)
	390(0.56)	402(0.62)	414(0.66)	429(0.45)	744(0.60)	758(0.50)	820(0.76)	840(1.0)
6	220(0.53)	236(0.41)	264(0.07)	278(0.06)	664(0.15)	680(0.18)	700(0.18)	728(0.36)
	390(0.53)	402(0.59)	414(0.63)	429(0.44)	744(0.55)	758(0.47)	820(0.71)	839(1.0)
7	220(0.46)	236(0.33)	264(0.06)	280(0.05)	664(0.14)	680(0.17)	700(0.17)	728(0.35)
	390(0.48)	402(0.56)	414(0.59)	430(0.40)	744(0.54)	756(0.46)	820(0.71)	839(1.0)
8	219(0.51)	236(0.33)	264(0.05)	280(0.05)	664(0.14)	680(0.17)	700(0.16)	728(0.35)
	390(0.47)	402(0.55)	414(0.59)	430(0.40)	744(0.54)	758(0.46)	820(0.71)	839(1.0)
9	221(0.53)	236(0.39)	264(0.08)	280(0.07)	664(0.14)	680(0.17)	700(0.17)	728(0.35)
	390(0.48)	403(0.56)	415(0.60)	430(0.41)	744(0.54)	758(0.46)	820(0.71)	839(1.0)
10	230(0.65)			280(0.08)	664(0.13)	680(0.17)	698(0.17)	726(0.32)
	390(0.57)	402(0.59)	416(0.59)	432(0.40)	744(0.57)	758(0.46)	822(0.70)	841(1.0)
12	226(1.33)	266(0.04)	278(0.08)		662(0.16)	680(0.18)	698(0.18)	726(0.33)
	370(0.78)	390(1.25)	414(0.70)	430(0.43)	744(0.55)	758(0.47)	820(0.69)	840(1.0)
15 <sup>a</sup>	217(0.58)	236(0.40)		280(0.07)	664(0.15)	678(0.19)	698(0.19)	728(0.36)
	389(0.53)	402(0.58)	414(0.62)	430(0.41)	744(0.57)	758(0.38)	820(0.72)	839(1.0)
16 <sup>b</sup>	228(0.10)		274(0.02)	310(0.03)				
	370(0.65)	390(1.0)						

<sup>a</sup> Synthesized CuTCNQ powder. <sup>b</sup> TCNQ.**Figure 6.** UV–vis spectra of the films **1** (solid line), **3** (dotted line), and **6** (dashed line) with the increase of exposure time from 1, 4, to 10 min. The spectra were recorded in acetonitrile solution, and the vertical axis refers to absorbance in arbitrary units.

nitrile solution showing relative absorbance for each absorption to the band at about 840 nm. Presentative electronic absorption spectra of some selected film materials are shown in Figure 6.

The electronic absorption spectra of the film materials agree well with those previously reported,<sup>21</sup> and also observed are the rather small differences of the spectra among the film materials. In the red-band region, the spectra of the films were characterized by three typical absorptions maxima at 680, 744, and  $840 \pm 1$  nm, respectively. The absorption maxima at  $840 \pm 1$  and 744 nm in the red-band system might represent separate electronic transitions to the first two doublet excited

(21) (a) Jeanmaire, D. L.; Van Duyne, R. P. *J. Am. Chem. Soc.* **1976**, *98*, 4029. (b) Boyd, R. H.; Phillips, W. D. *J. Chem. Phys.* **1965**, *43*, 2927. (c) Hiroma, S.; Kuroda, H.; Akamatu, H. *Bull. Chem. Soc. Jpn.* **1971**, *44*, 9.

states of TCNQ anion radicals and can be considered as the  $\text{CT}_1$  transition. The absorption maxima at 680 may be regarded as  $\text{LE}_1$  transition. In the whole, the red-band system may be assigned to the  ${}^2\text{B}_{2g} \rightarrow {}^2\text{B}_{1u}^{(1)}$  transition with fine structures located at around 664, 700, 728, 758, and 820 nm representing partially resolved vibronic transitions in terms of the theoretical work of Lowitz.<sup>22</sup> In the blue-band region, there is one typical absorption maxima at  $415 \pm 1$  nm ( $\text{LE}_2$  transition) and is assigned to contributions from both  ${}^2\text{B}_{2g} \rightarrow {}^2\text{B}_{1u}^{(2)}$  and the  ${}^2\text{B}_{2g} \rightarrow {}^2\text{A}_u$  transitions.<sup>22</sup> Partially resolved vibronic transitions are also evident in this band system; see Table 3 and Figure 6.

Comparing the spectra of the film materials with those of the synthesized pure CuTCNQ powder, one can note that the spectra of the CuTCNQ film materials are identical with that of the synthesized pure CuTCNQ powder. In addition, both the spectra of CuTCNQ films and the CuTCNQ powder in acetonitrile solution are identical with those of electrogenerated TCNQ anion radicals,<sup>21a</sup> LiTCNQ,<sup>21b</sup> and KTCNQ.<sup>21c</sup> They are all characterized by four major bands that appear at about  $840 \pm 1$ , 744, 680, and  $415 \pm 1$  nm. The strongest peaks are at  $415 \pm 1$  and  $840 \pm 1$  nm and occur with an average intensity ratio of about 0.65, which is typical of simple TCNQ anion radical salts with complete CT.<sup>11,23</sup>

TCNQ acetonitrile solution exhibits the well-known strong peak at ca. 390 nm,<sup>11,24</sup> which is assigned to the  ${}^1\text{A}_g \rightarrow {}^1\text{B}_{3u}$  (long axis polarized) transition.<sup>25,26</sup>

The optical absorption spectra of TCNQ-based CT compounds are related not only to the degree of CT in

(22) Lowitz, D. A. *J. Chem. Phys.* **1967**, *46*, 4698.

(23) Kamitsos, E. I.; Risen, Jr., W. M. *J. Chem. Phys.* **1983**, *79*, 5808.

(24) Acker, D. S.; Harder, R. J.; Hertler, W. R.; Mahler, W.; Melby, L. R.; Benson, R. E.; Mochel, W. E. *J. Am. Chem. Soc.* **1960**, *82*, 6408.

(25) Eckhardt, C. J.; Pennelly, R. R. *Chem. Phys. Lett.* **1971**, *9*, 572.

(26) Hiroma, S.; Kuroda, H.; Akamatu, H. *Bull. Chem. Soc. Jpn.* **1970**, *43*, 3626.

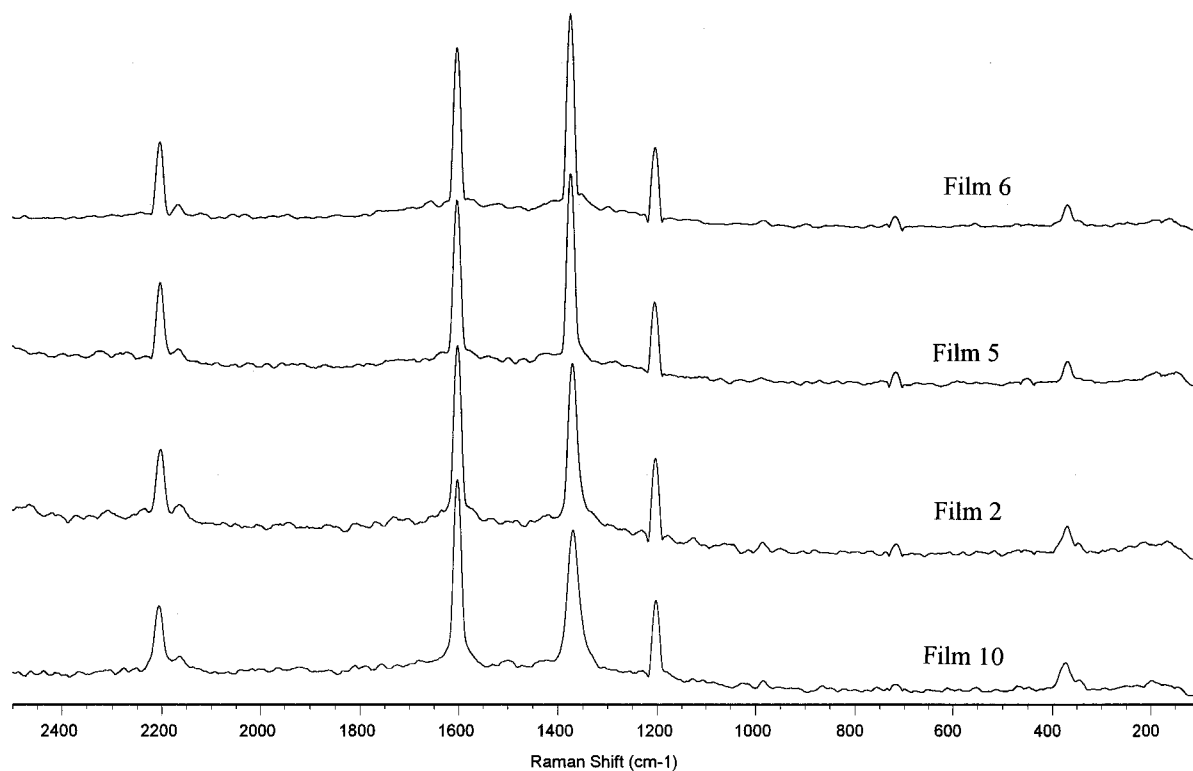


**Figure 7.** Raman spectra of the films **2**, **5**, **6**, and **10**. The vertical axis refers to Raman intensity in arbitrary units.

the compounds and thus to the remarkable electrical properties they exhibit but also to their resonance Raman spectra, as we now discuss.

**3.3.3. Raman Spectral Characteristics.** Raman spectroscopy has proven to be quite useful for studying TCNQ-based CT compounds. On one hand, since TCNQ is a centrosymmetric species and has strong sharp Raman-active modes, and of the most important is that some of the active modes are quite sensitive to the oxidation state of the TCNQ moiety in its CT compounds.<sup>27</sup> On the other hand, a measure of the degree of CT between donor and acceptor molecules, which is essential to understanding the conduction mechanism in the CT salts,<sup>28</sup> has been obtained in many cases from their Raman frequencies. This has been done by employing a linear relationship between vibrational frequency and charge density that was established on systems whose average charge per molecule can be determined stoichiometrically.<sup>29</sup>

Table 4 lists the Raman fundamentals of some selected CuTCNQ films and neutral TCNQ in the region 100–2500 cm<sup>-1</sup>. We can notice that four to seven Raman fundamentals were observed in this work in the region.<sup>30</sup>

It should be noted that excitation with the red-band 1064 nm line, gives quite a different spectrum from those excited with the blue-band 457.9, 476.5, and 514.5 nm lines.<sup>23</sup> In the spectrum, the bands around 980 and 715 cm<sup>-1</sup> are very weak, but the band around 1370 cm<sup>-1</sup> is the second or even the first strongest one, see Figure

**Table 4. Totally Symmetric Raman Fundamentals of Some Selected CuTCNQ Films and Neutral TCNQ in the 100–2500 cm<sup>-1</sup> Region**

film	$\nu_2$	$\nu_3$	$\nu_4$	$\nu_5$	$\nu_6$	$\nu_7$	$\nu_8$	$\nu_9$	$\nu_{10}$
2	2202	1602	1370	1203	985	715			368
5	2203	1603	1374	1204		716			372
6	2204	1603	1374	1203		717			367
8	2205	1604	1375	1204					367
10	2205	1603	1369	1202	984	716			372
12	2201	1597	1369	1200					
13	2203	1602	1373	1203	984	739	555	369	
16 <sup>a</sup>	2225	1600	1452	1205	946	709	591	333	154

<sup>a</sup> TCNQ.

7. Since the relative intensity of the 1370 cm<sup>-1</sup> band follows the red-band absorption while that of the 980 or 715 cm<sup>-1</sup> peak follows the blue-band system. The observed enhancement selectivity is due to the fact that these modes are coupled differently from the two different electronic excitations. Kamitsos et al.<sup>23</sup> reported that as the excitation changes from 457.9, 476.5, to 514.5 nm, the 1203, 980, and 734 cm<sup>-1</sup> bands decrease in relative intensity.<sup>23</sup> This may be explained from the fact that these wavelengths fall in the same (blue band) electronic absorption region of the CuTCNQ salt.

On the basis of the vibrational analysis of TCNQ anion radicals and other TCNQ salts, we can assign the bands of the CuTCNQ films at  $2203 \pm 2$ ,  $1601 \pm 3$ ,  $1372 \pm 3$ ,  $1202 \pm 2$ ,  $985 \pm 1$ ,  $716 \pm 1$ , and  $370 \pm 2$  cm<sup>-1</sup> to totally symmetric modes ( $A_g$ ), those analogous bands in  $TCNQ^0$  are at 2225, 1600, 1452, 1205, 946, 709, and 333 cm<sup>-1</sup>. Thus, the resonance Raman spectra of CuTCNQ films are completely dominated by the  $A_g$  modes of TCNQ anion radicals, and furthermore they show selectivity in resonance enhancement even among the totally symmetric modes, e.g., the ones at  $1372 \pm 3$  and  $716 \pm 1$  cm<sup>-1</sup>.

It is known that the  $\nu_3$  (C=C ring stretching) and  $\nu_5$  (C=C–H bending) modes are not much affected by

(27) Girlando, A.; Bozio, R.; Pecile, C. *Chem. Phys. Lett.* **1974**, *25*, 409.

(28) Torrance, J. B. *Acc. Chem. Res.* **1979**, *12*, 79.

(29) (a) Bozio, R.; Pecile, C. *The Physics and Chemistry of Low-Dimensional Solids*; Alcacer, L., Ed.; Reidel, Boston, 1980. (b) Matsuzaki, S.; Kuwata, R.; Toyoda, K. *Solid State Commun.* **1980**, *33*, 403.

(30) Bozio, R.; Girlando, A.; Pecile, C. *J. Chem. Soc., Faraday Trans. 2*, **1975**, *71*, 1237.

changes in the electronic structure of the TCNQ moiety, while the others, especially the  $\nu_4$  (C=C wing stretching) mode, are quite sensitive to these changes. In fact, a linear dependence of the stretching frequency of the  $\nu_4$  mode on the degree of CT ( $\rho$ ) between the donor and the acceptor TCNQ molecules was shown.<sup>31</sup> Thus, the degree of CT in the CuTCNQ thin-film materials can be estimated from the linear correlation between the wavenumbers of the  $\nu_4$  mode and the degree of CT. Since the intercept and the slope were experimentally determined to about 1450 and  $-65\text{ cm}^{-1}$ , respectively.

For pure TCNQ, the  $\nu_4$  mode exists at  $1452\text{ cm}^{-1}$  which corresponds to the state of no CT, i.e.,  $\rho = 0$ . In the cases of the CuTCNQ films, this mode exists at  $1372 \pm 3\text{ cm}^{-1}$ . The wavenumbers shifted from  $1452$  to  $1372 \pm 3\text{ cm}^{-1}$  through the formation of the CuTCNQ complex by means of the redox reaction between copper and TCNQ. In these cases, the degree of CT is estimated at about 1.0. This means that complete CT has happened between copper and TCNQ in the CuTCNQ films, which is in good accordance with the UV-vis spectral analysis.

To this point, we can conclude that changing the preparation methods or growth parameters does not significantly change the spectral properties of the CuTCNQ film materials and the unswitched form of the films studied is  $\text{Cu}^+\text{TCNQ}^-$  based on the spectral analyses of the film materials and those of  $\text{Cu}^+\text{TCNQ}^-$  powder prepared by the reaction of CuI and TCNQ.<sup>11</sup>

**3.4. Electrical Switching and Mechanism.** Dc current–voltage ( $I$ – $V$ ) characteristics were measured as described in literatures.<sup>14,15</sup> We did not attempt to make switching measurements on all the films prepared in this study. Rather we chose some presentative film samples, such as films **2**, **6**, **8**, **11**, **13**, and **14** and observe the switching effect. The switching property of the films **11** and **14** were reported in the literature.<sup>14,15</sup> We report here the electrical switching behavior of films **2**, **6**, **8**, and **13**. While it is desirable to measure the film **12** which was grown in 1-bromohexadecane, the film did not adhere well to the copper substrate. As a result, reliable switching measurements on the film were not obtained and are not reported.

For film **6**, threshold and memory behavior are observed by examining current as a function of voltage across the two terminal structures. Figure 8 presents a typical OFF–ON dc  $I$ – $V$  curve for a Al/CuTCNQ/Cu system. It shows that there are one stable ohmic and one stable nonohmic resistive states in the material. At the outset, the device was in the high-impedance OFF state ( $1.5 \times 10^5\text{ }\Omega$ ). When the applied voltage exceeded a certain threshold, the device resistance abruptly decreased to about  $1.4 \times 10^2\text{ }\Omega$ , thus putting the device into the low-impedance ON state. As the applied voltage was lowered to zero, the device impedance was almost unaltered so that true memory switching behavior was observed. These two states, called OFF state and ON state, are essentially insensitive to air, moisture, light, and the polarity of the applied voltage. A rapid switching is observed from the OFF to the ON state along the load line when an applied field across the sample surpasses a  $V_{th}$  of 15 V. This corresponds to a field strength of about  $7.5 \times 10^4\text{ V cm}^{-1}$  for a 20

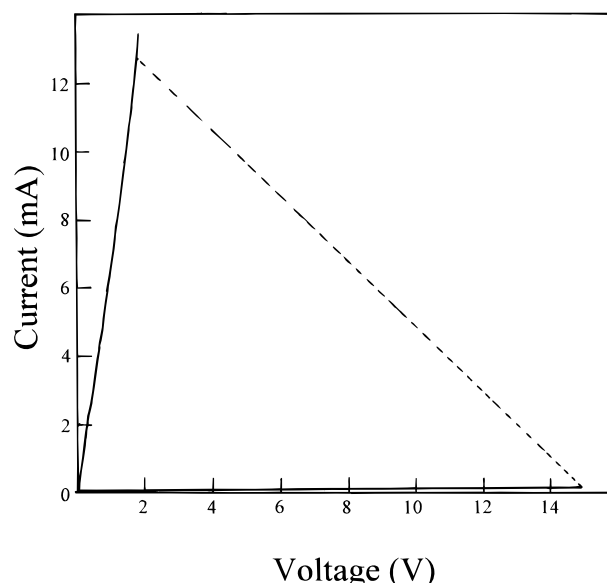


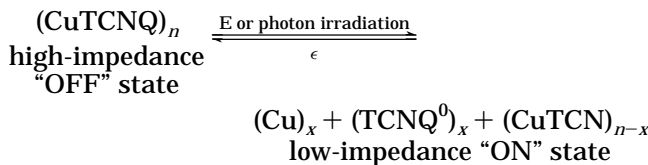
**Figure 8.** Typical dc  $I$ – $V$  characteristic curve showing the high- and low-impedance states for a  $20\text{ }\mu\text{m}$  thick CuTCNQ film.

$\mu\text{m}$  thick film material. At this field strength, the initial high-impedance state of the device decreases to a low impedance state. A rise in current from about  $0.1\text{ mA}$  to approximately  $12.7\text{ mA}$  and a concurrent drop in the voltage to  $1.8\text{ V}$  along the load line is observed in the system. In addition, it has been observed that once the device is in the ON state, it will remain in that state as long as an external field is applied. In every cases studied, the device eventually returned to its initial high-impedance state after the applied field was removed, which is called a memory effect, i.e., memory state. This memory state can remain intact from a few minutes to several hours after the applied potential was removed, and it can be also immediately driven back to the OFF state by application of large currents in either direction. The current required to switch back to the initial OFF state appeared to be directly proportional to the duration of the applied field in the ON state and the amount of power dissipated in the device while in this state. These results are consistent with those of Potember et al.,<sup>1</sup> where the polarity is unimportant, and the device could be switched OFF by the application of large currents in either direction.

It should be pointed out that similar phenomenon could be observed in other film materials studied and the  $V_{th}$  values for all the systems investigated are reasonably constant and independent of the film thickness. However, those films with loosely packed structure cause some serious problems in the fabrication process of the devices. Of the most serious is the penetration problem of the top metal electrode when it was deposited on the surface of the film under vacuum and hence this may cause a short circuit in the complete device. In fact, in our fabrication processes and  $I$ – $V$  measurements, we have observed this short-circuit phenomenon on some points. The reasonably constant  $V_{th}$  values indicate that changing the preparation methods or growth parameters does not significantly change the electronic properties of the complete devices. This may be explained by the fact that the switching phenomenon is a bulk property of the CuTCNQ complex and the magnitude of the applied field

(31) Kamiratos, E. I.; Tzinis, C. H.; Risen, Jr. W. M. *Solid State Commun.* **1982**, *42*, 561.

strength required to cause switching only depends on the strength of the  $\pi$ -electron acceptor. These results seem to support the mechanism reported by Potember et al.,<sup>32</sup> quoted as follows:



The reaction shown is reversible by adding energy  $\epsilon$ , which can be in the form of heat, electric field, or photon irradiation under different conditions.

However, Sato et al. reported that the switching phenomena may be analyzed from the viewpoint of the bulk and contact property.<sup>10</sup> In other words, the contacts between the Al electrode and the CuTCNQ film are considered to play an essential role in the polarized memory effect observed in their work and this interest is supported by the experimental fact that they could not observe the switching effect when other electrode metals such as nickel or gold were employed in place of aluminum.<sup>10</sup> While this is contrasted to the results reported by Kamitsos et al.,<sup>31</sup> where Cr or SnO<sub>2</sub> was used as the top electrode in place of Al, but a switching effect could also be observed and even more the neutral TCNQ produced on switching to the ON state was detected by Raman spectral analysis, which seems to be direct evidence to support the mechanism shown above. Now, a question arises as to why different authors reported different results? This may be a very complicated question to be answered now because the structure of the CuTCNQ crystal has not yet been known. Maybe the arrangement of the TCNQ anion or copper cation in the CuTCNQ crystal can affect significantly the switching behavior of the devices composed

(32) (a) Potember, R. S.; Pochler, T. O.; Cowan, D. O.; Brant, P.; Carter, F. L.; Bloch, A. N. *Chem. Scr.* **1980**, *17*, 219. (b) Potember, R. S.; Pochler, T. O.; Cowan, D. O.; Carter, F. L.; Brant, P. *Molecular Electronic Devices*; Carter, F. L., Ed.; Marcel Dekker: New York, 1982; p 73. (c) Potember, R. S.; Pochler, T. O.; Hoffman, R. C.; Speck, K. R. *Molecular Electronic Devices II*; Carter, F. L., Ed.; Marcel Dekker: New York, 1987; p 91. (d) Yamaguchi, S.; Viands, C. A.; Potember, R. S. *J. Vac. Sci. Technol. B9*, 1129.

of CuTCNQ complex. So even if the preparation parameters significantly change the morphology of the resulting film materials but not lead to significant changes in the structure, the switching behavior may not differ significantly. While if slight changes in the preparation conditions lead to some changes in the structure, the switching property may differ significantly. There is a lot of work to be done to clarify this point of view.

#### 4. Conclusions

In summary, a series of CuTCNQ film materials were prepared by three different methods and characterized by SEM and IR, UV-vis, and Raman spectral analyses as well as *I*–*V* measurements. The spectral analyses were compared with those of synthesized pure CuTCNQ powder produced by the reaction of CuI and TCNQ, and thus it is concluded that the unswitched form of the film materials studied is Cu<sup>+</sup>TCNQ<sup>–</sup> with complete charge transfer between Cu and TCNQ based on the spectral analyses of the film materials and those of Cu<sup>+</sup>TCNQ<sup>–</sup> powder, and changing the preparation methods or growth parameters can significantly change the morphologies of the resulting film materials; however, these morphological changes do not lead to significant changes in their spectral characteristics and the electronic properties of the complete devices in this study. *I*–*V* curves showed that memory switching phenomena can be observed for the film materials sandwiched between Al and Cu electrodes. The switching is independent of the polarity of the applied potentials and the threshold voltage does not depend on the film thickness, and it can be identified as an electric field induced solid-state redox reaction with the fact that the magnitude of the applied field strength required to cause switching depends only on the strength of the  $\pi$ -electron acceptor. These properties combined with the ability of preparing the materials in the form of thin films may give them a special technological importance.

**Acknowledgment.** The work was supported by the Key Funds of the Chinese Academy of Sciences and NNSFC.

CM9602656